Biosensors and Bioelectronics 44 (2013) 164–170

Contents lists available at SciVerse ScienceDirect

Biosensors and Bioelectronics

journal homepage: www.elsevier.com/locate/bios

Direct label free ultrasensitive impedimetric DNA biosensor using dendrimer functionalized GaN nanowires

Prasana Sahoo [a,*], Sumathi Suresh [b], Sandip Dhara [a,*], Garima Saini [c], S. Rangarajan [b], A.K. Tyagi [a]

[a] Surface and Nanoscience Division, Indira Gandhi Center for Atomic Research, Kalpakkam, India
[b] WSCD, BARC Facilities, Indira Gandhi Center for Atomic Research, Kalpakkam, India
[c] National Institute Technology, Kurukskhetra, India

ARTICLE INFO

Article history:
Received 10 December 2012
Accepted 11 January 2013
Available online 8 February 2013

Keywords:
Gallium nitride nanowire
DNA
Biosensor
SWINE flu (H1N1)
In-situ detection
Dendrimer

ABSTRACT

We demonstrate a very simple and generic protocol for ultrasensitive in-situ label-free detection of DNA hybridization using third generation poly(amidoamine)dendrimer (G3-PAMAM) functionalized GaN nanowires (NWs). PAMAM modified GaN NWs provides large density of docking site to immobilize significant number of probe (p-) DNA covalently. These p-DNA/PAMAM/GaN NWs sensor probes are employed to achieve an ultra-high detection limit down to attomolar level concentration of complementary target (t-) DNA. Comparative in-situ studies on single/triple base-pair mismatched, γ-irradiated and complementary t-DNA in the hybridization process reveal selectivity and specificity of the p-DNA/PAMAM/GAN NWs sensor probe over a wide range, 10^{-8} to 10^{-19} M, of analyte concentration. During the hybridization process, there is a substantial change in t-DNA concentration dependent interfacial polarization resistance during electrochemical impedance measurement, which forms the basis of the present DNA biosensor. This novel methodology for specific DNA sequence detection, as compared with the existing methods, is found to be very robust, highly sensitive, and reproducible.

© 2013 Elsevier B.V. All rights reserved.

1. Introduction

Nanowires (NWs) have emerged as one of the promising class of functional materials for their versatile roles, not only in high throughput optoelectronic devices but also in ultrasensitive, direct electrical detection of biological and chemical species (Sahoo et al., 2011a; Patolsky and Lieber, 2005; Wang et al., 2005 and Cui et al., 2001). Compared to thin film counterpart, NWs possess large surface-to-volume ratio, unidirectional conduction channels, and diameters comparable to the sizes of molecules being sensed. These aspects have generated considerable interest to use NWs as an effective bioelectrochemical transducer. Remarkably, the conductance in NWs is very sensitive to small surface perturbations (Grieshaber et al., 2008). The NW based field-effect-transistor (FET) is most widely used for biosensing purposes, such as the detection of particular DNA sequence, pH, protein, viral and cancer markers (Cui et al., 2001 and Wang et al., 2005). However, progress in successful implementation of FET based NW biosensing devices are hindered by several challenges. Without the requirement of expensive instruments and reagents, NWs based electrochemical sensing techniques, can allow in-situ, real-time, non-destructive, and label-free detection of the specific biomolecule of interest by appropriate control over the physical properties and surface functionality (Wanekaya et al., 2006; Wang 2006; Feigel et al., 2011; Pérez et al., 2011 and Chen et al., 2009). These materials also appear to be superior than polypyrrole-modified electrode, bio-conducting polymer-Nile blue composite electrode and conducting polymers based DNA sensors (Ramanaviciene and Ramanavicius, 2004; Peng et al., 2009; Chen et al., 2009; Teles and Fonseca, 2008).

Direct and wide band gap GaN NW is known to have high carrier mobility, chemical robustness, biocompatibility, and high spatial separation of charge carriers. These properties bestow it in diversity of applications pertaining to high efficient optoelectronic, biomedical devices and sensors (Sahoo et al., 2011a). However, most of the reports on GaN based applications in biosensing are limited to the thin film configuration; for example GaN based planar transistor has been reported to detect specific DNA sequence, changes in pH, glucose, and even detecting proteins associated with breast cancer (Ren et al., 2011 and Kang et al., 2006). Nonetheless, GaN NWs based DNA sensor has been recently

* Corresponding authors. Tel.: +91-44-27480500-(extn) 22513, 22083.
E-mail addresses: prasanasahoo@gmail.com (P. Sahoo), dhara@igcar.gov.in (S. Dhara).

0956-5663/$ - see front matter © 2013 Elsevier B.V. All rights reserved.
http://dx.doi.org/10.1016/j.bios.2013.01.023

demonstrated employing 3-merkapto-tri-methoxy-silane functionalized GaN NWs as working electrode in the electrochemical impedance spectroscopy (EIS) technique (Chen et al. 2009,2011). Moreover, the sensitivity and stability of DNA biosensor can be enriched by modulating the surface chemistry and choosing appropriate tether molecule in order to generate multiple docking sites to immobilize significant amount of probe (p-) DNA molecules. In this context, dendrimer can be able to serve as a tether for surface confinement of the large amount of probe DNA (Zhu et al., 2010,2006). It was demonstrated that fourth generation poly(-amidoamine)dendrimer (G4-PAMAM) modified Au electrode increases the sensitivity of the electrochemical based DNA biosensor (Zhu et al., 2006; Li et al., 2009). Similar behavior is observed for (PAMAM) modified carbon nanotubes (CNT) dip coated onto a glassy carbon electrode (Zhu et al., 2010). However, in most of the cases the maximum achievable detection of target (t-)DNA is traced down to few fM levels. Several factors limit the ultra-low detection capability, which includes the difficulties involved in (1) separating metallic and semiconducting CNTs because metallic components do not function like semiconductor counterpart, (2) selective surface modification of CNT for binding a wide range of analytes, and (3) appropriate interface with the read out system for both CNT and Au nanoparticle based sensor probe. Thus, it is expected that integration of dendrimer based surface chemistry onto NWs based electrode will lower the detection limit of the electrochemical DNA biosensing.

We have demonstrated a very simple and generic protocol for ultrasensitive in-situ label-free detection of DNA hybridization with high degree of selectivity and specificity. The strategy employed here is based on the combination of advantages gained from both GaN NWs grown directly over heavily doped Si substrate and functionalization with G3-PAMAM dendrimer. Notably, current approach towards biosensor is focused on single nanowire based devices (Patolsky and Lieber, 2005 and Wang et al., 2005). The cost and difficulties involved in the integration of individual NWs into thin-film-based sensor-chips can be simplified by using as-synthesized NWs directly after appropriate surface modification. A correlated DNA sequence of influenza A (H1N1) Swine flu virus (24 base pair) has been employed as a model. The human influenza A (H1N1) virus corresponds to the orthomyxoviridae family, which is still creating pandemic concern as of now (Yang et al., 2009 and World Health Organization, 2009). One of the maximum used laboratory tests for confirmation of novel influenza A (H1N1) cases are based on real-time reverse transcription-polymer chain reaction (Wang et al., 2009). Other methodologies, based on antigen, immune-fluorescence or viral culture, are also often used (Bonanni et al., 2010). However, impedance based detection can also provide a parallel and consistent response. Our approach appears to be user friendly both in fabrication, as well as in achieving sensitivity and specificity over wide range of DNA detection. Finally, a realistic picture of DNA sensing methodology at the semiconductor and electrolyte interface are discussed.

2. Experimental methods

All chemical reagents and methodologies used for this study are detailed in the supplementary information. The GaN NWs are grown over 3 nm Au coated heavily doped Si substrate (n^+-type) by chemical-vapor-deposition technique which can be found from our earlier published paper (Sahoo et al., 2010).

2.1. Surface functionalization of NWs

Prior to DNA sensing, a series of functionalization steps were employed over NWs. Initially, GaN NWs were treated with Piranha solution (H_2SO_4:H_2O_2 3:1) for a period of 10 min, and then washed with double distilled water followed by drying with N_2 gas. This process generates hydroxyl group on the surface of the NW. The hydroxylated samples were further treated with 5 ml of H_2O solution containing 1 mM of 1,10-decanedicarboxylic acid for 6 h under gently stirring condition and washed three times with deionized water to remove all residual acids and dried with N_2 gas. This process generates –COOH functional group on the GaN surface (Lao et al., 2007). For dendrimer functionalization, COOH terminated NWs were mixed with 2 mg/ml G3-PAMAM solution containing 1 mM 1-ethyl-3-(3-dimethylaminopropyl) carbodimide (EDC) for 8 h at room temperature under gentle stirring which leaves the surface with NH_2 groups. Then, the samples were washed three times with deionized water as linker to p-DNA.

2.2. DNA protocol

The probe DNA (p-DNA) and ct-DNA used for this experiment are adopted from H1N1 Swine flu gene. The DNA protocols used in this study are enlisted as follows:

PO_4-DNA: (p-DNA)	PO_4-5′–TGC AGT CCT CGC TCA CTG GGCACG–3′
Complementary t-DNA: (ct-DNA)	3′–ACG TCA GGA GCG AGT GAC CCG TGC–5′
Single mismatch t-DNA: (sm-DNA)	3′–**G**CG TCA GGA GCG AGT GAC CCG TGC–5′
Triple mismatch t-DNA: (tm-DNA)	3′–**TA**G TCA GGA GCG AGT GAC CCG TG**A**–5′

All the oligonucleotides were high-performance liquid chromatography (HPLC) purified for accuracy in the measurement system, and purchased from Metabion International Matrinsried Deutschland, Germany. The DNA stock solutions were prepared with TE buffer solution (10 mM Tris–HCl and 1 mM ethylenediaminetetraacetate) with pH 8.0, and stored in freezer below 0 °C while not in use.

2.3. DNA probe immobilization

The p-DNA immobilized surface is a necessary step to selectively detect ct-DNA during hybridization process. The G3-PAMAM-modified GaN NWs were incubated in 10 nM of p-DNA (diluted in 1 mM TE buffer) solution containing 1 mM EDC for 12 h at room temperature to immobilize the p-DNA on the GaN surface. The p-DNA modified substrates were finally rinsed with 1 mM phosphate buffer solution followed by double distilled water to remove non-specific adsorbed molecules. These p-DNA/PAMAM/GaN NWs modified electrode were used for in-situ sensing of different t-DNA molecules.

2.4. In-situ detection of DNA hybridization

The in-situ impedance study of DNA hybridization was performed using the p-DNA/PAMAM/GaN NWs electrode within 10 mL of duplex buffer solution medium as the background electrolyte in the EIS technique (Eco Chemie Autolab PG STAT 30). Duplex buffer was used to maintain a constant pH (7.5) and the ion concentrations of these solutions generally match those of the human body. For in-situ measurement, ct-DNA of various concentrations ranging from 10^{-9} to 10^{-19} M levels were added slowly and allowed to hybridize for 2 h at RT and simultaneously the impedance spectra were recorded at a stable open circuit

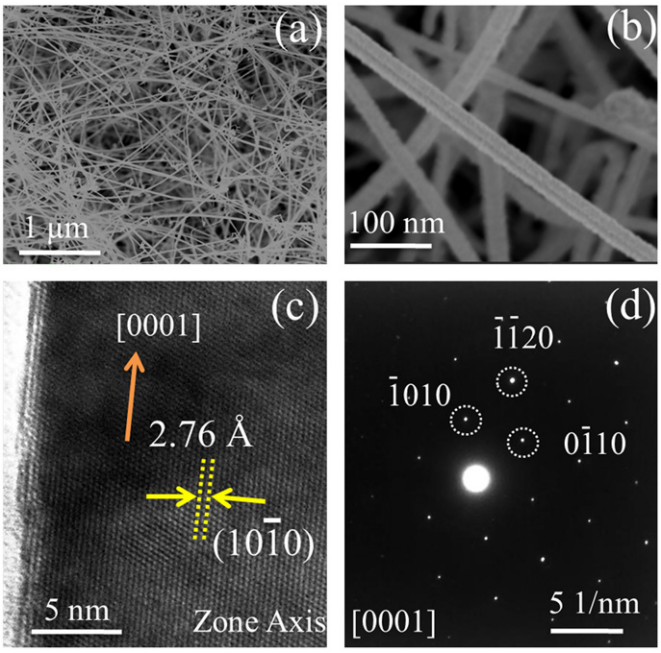

Fig. 1. (a) FESEM image of GaN NWs grown in Si substrates, (b) corresponding high magnification image; (c) HRTEM images of a single NW subtended along the [0001] direction of *wz*-GaN, (d) corresponding SAED pattern of the NW obtained along $<0001>$ zone axis of *wz*-GaN phase.

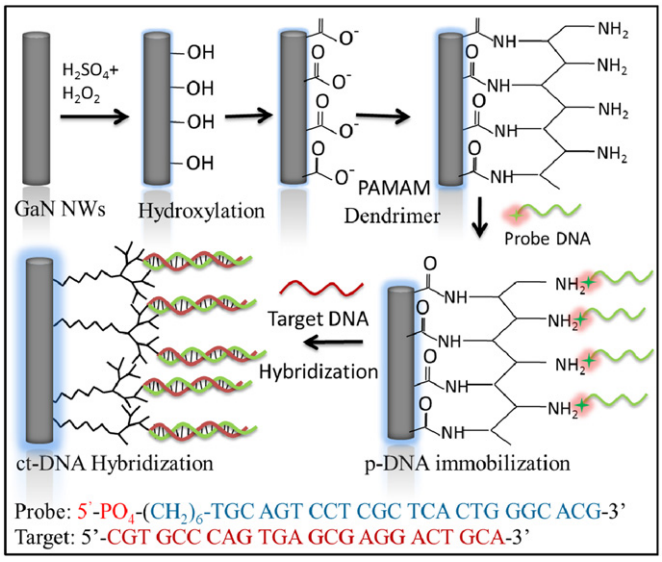

Fig. 2. Schematic representation showing all the series of functionalization steps involved for immobilization and hybridization of specific DNA on the PAMAM dendrimer functionalized GaN NWs.

potential with the application of a sinusoidal voltage of amplitude ± 10 mV in the frequency range of 100–0.005 Hz. The selectivity of the sensor probe was performed in the same procedure by adding single and triple base-pair mis-matched t-DNA of various concentrations. The specificity of the sensor probe, subjected to any radiation induced damage, was studied by monitoring the hybridization response from the γ-irradiated ct-DNA sequence. γ-ray doses of 1 Gy and 10 Gy were carried out over the ct-DNA from a Co-60 Gamma Chamber-900 source.

3. Characterization

Typical field emission scanning electron microscopy (FESEM; Model Zeiss SUPRA 40) image of NWs grown over Si substrate is shown in Fig. 1(a). The as-synthesized NWs possess uniform cylindrical shape morphology with an average diameter of ~20 nm and extended up to several tens of micrometers in length [Fig. 1(b)]. High-resolution transmission electron microscopy (HRTEM; Libra 200 Zeiss) analysis reveals that the NWs are single crystalline in character and subtended along [0001] direction of wurtzite (*wz*) GaN phase [Fig. 1(c)]. The corresponding selected area electron diffraction (SAED) pattern is indexed to $<0001>$ zone axis of *wz*-GaN [Fig. 1(d)]. The above studies reveal that the as-synthesized NWs are well crystalline in nature and possess smooth surface morphology.

The detailed surface modification steps and subsequent DNA hybridization process are schematically illustrated in Fig. 2. PL and Raman spectroscopic (inVia Renishaw spectrometer) studies are performed to ensure the covalent bonding of the functional groups with the NW surface molecules. Fig. 3(a) shows the typical PL spectra of NWs with subsequent surface modification. Room temperature PL spectrum of pristine GaN NWs is composed of two broad peaks around 3.46 and 3.29 eV. The peak at 3.46 eV corresponds to recombination of exciton bound to neutral donor (I_2) line. The broad peak at 3.25 eV corresponds to recombination of carriers from a shallow donor state [N_2 vacancy (V_N)] to a deep accepter state (DAP line). These two peaks are consistent with the PL figure print of GaN (Sahoo et al., 2012, Sahoo et al., 2011b). PL spectra of NWs recorded at 100 K show an expected blue shift with increase in intensities of the corresponding bands. In order to confirm the presence of functional groups on the NW surface, all the PL spectra are recorded at 100 K. Low temperature measurements have been performed to avoid secondary effect on functional groups induced by local heating upon incident with laser light. It is observed that the band edge emission has not been significantly affected by the chemical modification. However, the DAP emission band has shown spectacular variation with every stage of chemical functionalization process. The DAP line is blue shifted and intensity gets enhanced after hydroxylation process on NW samples. It may arise because of surface state passivation during the acidic treatment, which helps in removing the absorbed oxygen and surface defects from NW surface. Subsequent enhancement in the intensity of DAP line is also observed during carboxylic acid treatment followed by the dendrimer modification on the hydroxylated surface. Notably, the DAP peaks are red shifted compared to hydroxylated sample. With subsequent p-DNA modification, the DAP line is enhanced by three times of magnitude, and further red-shifted by 170 meV as compared to the pristine NWs at 100 K. A new shoulder at 2.9 eV appears only in case of DNA modified sample. The formation of DNA molecular layer on functional NW surface would have helped in activating the blue band at 2.9 eV and amplified further after the hybridization process. Moreover, the observed enhancement in PL intensity and band shift in GaN NWs substantiates the covalent attachment of the functional molecules on the NW surface. A schematic representation of the detailed transition state in functional GaN NWs, before and after DNA modification steps has been depicted in Fig. 3(b). The molecular orbitals of organic layers may have generated multiple radiative states in the proximity of DAP transition level.

The DNA modification on the NW surface is further confirmed by Raman spectroscopy. Typical micro-Raman spectra of control NWs [Fig. 3(c)] reveal four symmetry allowed modes with frequencies around 531, 547, 567 and 725 cm^{-1}, which

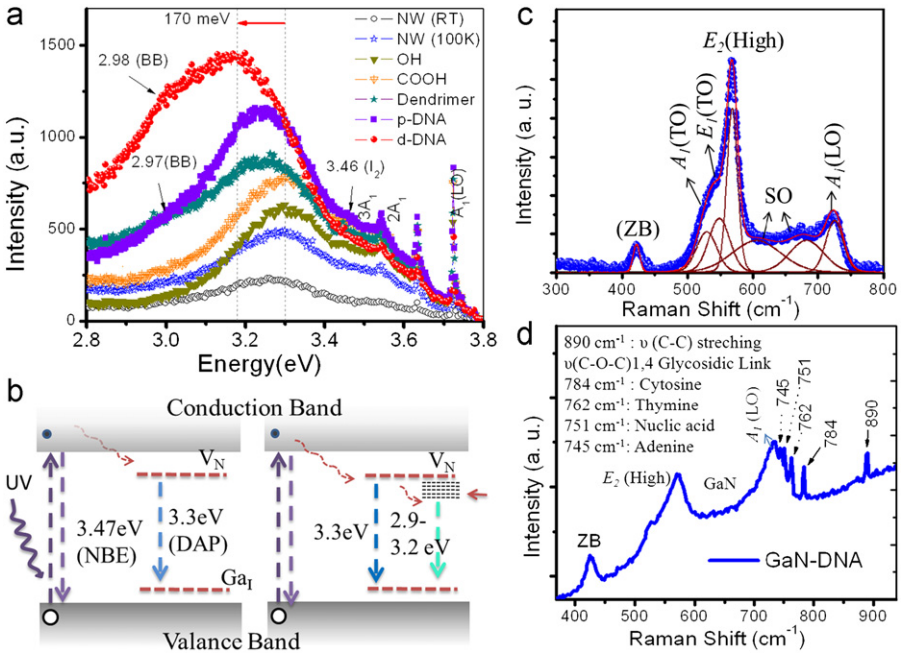

Fig. 3. (a) Low temperature micro-PL spectra of GaN NWs functionalized with different bioorganic molecules and DNA using 325 nm laser excitation; (b) Schematic PL band diagram of the various transition processes involved before and after surface functionalization of NWs; Raman spectra of (c) pristine GaN NWs and (d) after immobilization with p-DNA molecules.

correspond to A_1(TO), E_1(TO), E_2(High) and A_1(LO) phonon modes of *wz*-GaN phase, respectively (Sahoo et al., 2010). The peak at 421 cm^{-1} corresponds to zone boundary (ZB) phonon. Two additional peaks at 610 and 690 cm^{-1} may have originated from surface disorder induced surface optical (SO) modes (Sahoo et al., 2010). Along with characteristic features of GaN, the typical Raman spectrum of p-DNA modified GaN NW [Fig. 3(d)] shows additional phonon modes at 745 cm^{-1} (Adenine), 751 cm^{-1} (nucleic acid), 784 cm^{-1} (cytosine) and 890 cm^{-1} [ν C–C starching, ν (C–O–C) 1,4 glycosidic link] (Synytsya et al., 2007). These additional peaks correspond to various vibrational modes of DNA base pairs providing proof for the necessary immobilization of p-DNA on GaN NW surface.

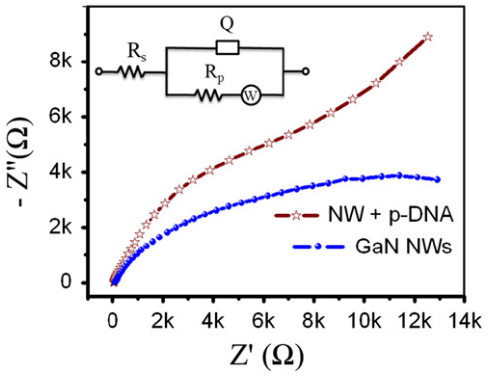

Fig. 4. Nyquist plots, imaginary impedance Z′′(Ω) vs. real impedance Z′(Ω), of pristine GaN NWs and p-DNA modified NWs. Inset shows the Randles equivalent circuit comprised of solution resistance R_s, polarization resistance R_p, constant phase element Q and Warburg resistance W.

4. Result and discussion

4.1. In-situ detection of H1N1 DNA sequence

EIS is an effective and simple technique both for understanding the nature of surface-modified electrodes and for analytical applications. The choice of semiconductor as electrode is advantageous over metal-based electrode in terms of surface band bending and reduced electron transfer rate across the interface between analyte and electrode (Grieshaber et al., 2008 and Wanekaya et al., 2006). In-situ detection of the DNA-hybridization process is carried out by employing the p-DNA/PAMAM/GaN NWs as working electrode in the EIS technique and using the duplex buffer as a support medium without using any redox marker. The main advantage of EIS is that it allows the use of a purely electronic model to represent an electrochemical cell. Thus, any electrochemical interface can be considered as a specific combination of resistors, capacitors, and inductors and characterized in terms of an equivalent circuit. Once a particular model is chosen, the physical or chemical properties can be correlated with the circuit elements. The electrical resistance and capacitance of a surface are sensitive indicators for changes of the surface properties and therewith for the detection of DNA hybridization.

The Nyquist plots, imaginary impedance Z′′(Ω) vs. real impedance Z′(Ω), of pristine GaN NWs and p-DNA modified NWs are shown in Fig. 4. The impedance spectra are constituted by semicircle at low frequency side (electron-transfer-dominated process) and a 45° inclined line at higher frequency side (diffusion-limited process; Daniels and Pourmand, 2007 and Lisdat and Schafer, 2008). It shows typical nonfaradaic type behavior. For this situation, a Randles equivalent circuit is used as shown in the inset of Fig. 4. It comprises of solution resistance R_s, polarization resistance R_p, a constant phase element Q for better fitting for some of the elements instead of true capacitance (generally used due to the electrode surface non-idealities) and Warburg impedance W. Impedance due to Q is expressed as $Z_Q = 1/Y_o(j\omega)^{-n}$ where Y_o is the magnitude of the Q, ω is the angular frequency and n the exponential term of the Q. The value of R_p has been used

as the parameter of interest for the present impedimetric DNA sensor. Fig. 4 reveals that the R_p value increases after p-DNA immobilization over PAMAM/GaN NWs tether. Remarkably, the interfacial diffusion related process is suppressed in case of pristine GaN NWs. The increase in the value of R_p and appearance of strong tail in the impedance spectra of p-DNA/PAMAM/GaN NWs electrode reveals that there is an efficient charge transfer process occurs owing to the strong covalent biobinding on the NW surface.

Prior to the in-situ hybridization process, the stability of p-DNA/PAMAM/GaN NWs electrode in the duplex buffer environment has examined over 24 h without any addition of t-DNA solution to observe any noticeable change occurring over R_p value (Supplementary information Fig. S1). It is found that this sensor probe provides a stable R_p value over a substantial time without any damage or leaching out of functional materials from the surface of the electrode. Further, addition of ct-DNA (1 pM concentration) onto the solution containing p-DNA probe, a significant change in the impedance spectra is observed within a period of 2–3 h and which ultimately saturates (Supplementary information Fig. S1). On this basis, the optimum saturation time for the DNA hybridization has been taken as 2 h for carrying out further in-situ detection of t-DNA over a wide range of concentration. The in-situ DNA hybridization is performed by monitoring impedance spectra of the p-DNA/PAMAM/GaN NWs electrodes thereby adding the ct-DNA solution subsequently in the hybridization buffer over a range of 0.1×10^{-18} to 10×10^{-9} M concentration after each 2.30 h followed by mild purging with Ar gas.

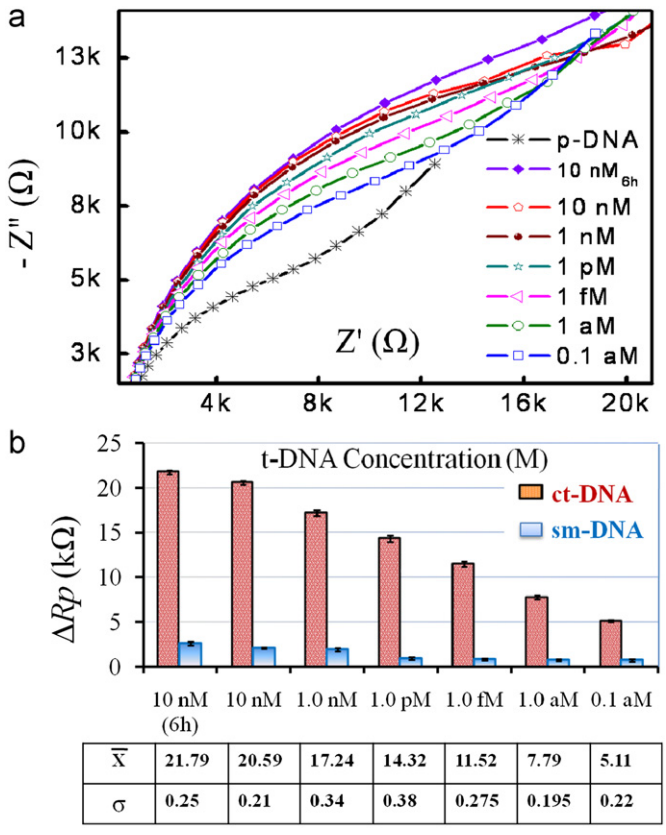

$\overline{X}$	21.79	20.59	17.24	14.32	11.52	7.79	5.11
σ	0.25	0.21	0.34	0.38	0.275	0.195	0.22

Fig. 5. (a) In-situ impedance spectra of the p-DNA/PAMAM/GaN NWs sensor probe during the hybridization process by varying the ct-DNA concentration over a range of 0.1×10^{-18} to 10×10^{-9} M level at a constant OCP value; (b) Comparative bar diagram deviation showing the relative change (Δ) in R_p with mean value and standard deviation of the p-DNA/PAMAM/GaN NWs sensor probe against various concentrations of ct-DNA and sm-DNA.

The impedance spectra are recorded after a period of 2 h from the addition of fresh ct-DNA solution into the hybridization buffer. Fig. 5(a) displays the in-situ Nyquist plots for the DNA hybridized process over 0.1 aM–10 nM of ct-DNA concentration at a constant OCP value. It is observed that the R_p value increase with the increase in the concentration of ct-DNA because of hybridization process. Remarkably, the detection of ct-DNA sequence is more pronounced and linear at low concentration level (aM–pM) while the change in the R_p value is low at high concentration. At higher concentration, secondary processes such as steric hindrance, coulomb repulsion, over population of ct-DNA, or reduction of DNA binding sites might have affected the in-situ hybridization process.

4.2. Selectivity and specificity

To evaluate the selectivity of the impedimetric DNA biosensor, the p-DNA/PAMAM/GaN NWs electrodes are incubated in the hybridization buffer containing different kinds of t-DNA molecules including single base mismatched (sm-DNA) and triple base mismatch (tm-DNA). An insignificant change in R_p value is observed when the p-DNA/PAMAM/GaN NWs electrode is subjected to incubate in the hybridization buffer containing the sm-DNA [Fig. 5(b)] and no change in case of tm-DNA (not shown in figure). It shows that any nonspecific adsorption of non-complementary DNA has negligible effect on DNA hybridization. Thus, it endorses the excellent selectivity nature of the p-DNA/PAMAM/GaN NWs sensor probe. This has been clearly elucidated in the bar diagram in Fig. 5(b) with mean value (QUOTE $\overline{X}$) and standard deviation (σ), taking into account of the relative change in R_p value of the sensor probe against various concentration of ct-DNA and sm-DNA. On the other hand, the specificity of the probe sensor has been examined from the viewpoint of damaged ct-DNA role in the hybridization process (Supplementary information Fig. S2). The impedance spectra are examined over a period of 5 h for different doses of γ-irradiated (1–10 Gy) ct-DNA. The ct-DNA base pair, upon irradiation with high ionized γ-rays, is not participating in the hybridization process. In fact, highly ionized irradiation would induce secondary effect on the DNA sequence, such as, alteration to the bases, rupture of the strand, destruction of the sugars, cross-linking, and formation of dimers (Synytsya et al., 2007). Hence, it is expected that ct-DNA undergoes significant change in its physiological properties after highly ionized irradiation and hence does not take part in the hybridization process. These results demonstrate that the changes of the R_p value of the electrochemical DNA biosensors are induced by the specific hybridization process between the p-DNA/PAMAM/GaN NWs sensor probe and the t-DNA in duplex buffer medium. In addition, the impedance response of the sensor probe remains unchanged after measuring the impedance parameter of same sensor probe after more than 1 week while stored in PBS buffer. This indicates that the present methodology for realizing a label-free DNA biosensor has good reproducibility, and stability characteristics.

4.3. Mechanism of DNA sensing using EIS

The DNA sensing mechanism can be well understood from the viewpoint of band offset at the hetero-interfaces formed at the semiconductor/bioorganic layer as depicted schematically in Fig. 6(a). Generally, an interface dipole layer (IDP) develops at the interface when a semiconductor surface meets electrolyte/bioorganic layers owing to the formation of heteronuclear bonds (Stutzmann et al., 2006). The formation of IDP layer is responsible

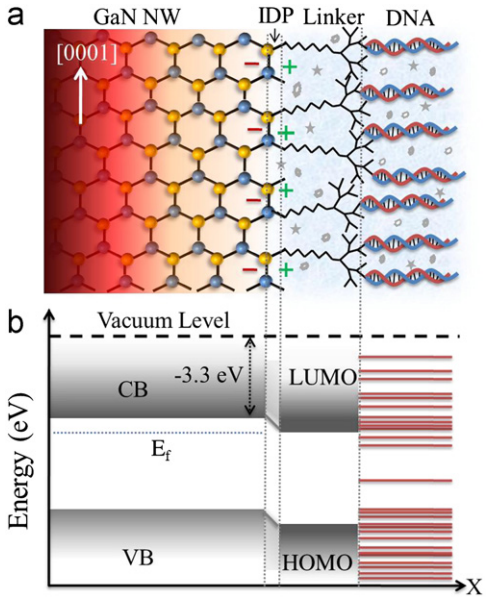

Fig. 6. (a) Schematic illustration of the hetero-interfaces formed at the interface between GaN NWs and bioorganic layer; (b) the corresponding band diagram of GaN NWs and the molecular orbitals, namely HOMO and LUMO levels of the organic linker and the DNA molecules.

for hopping of the localized carriers along the gradient of electrostatic potential across the interface. On the other hand, the electronic properties of the linker molecules depend on the respective molecular electronic states, namely highest occupied molecular orbital (HOMO) and the lowest unoccupied molecular orbital (LUMO). Whereas, for the case of DNA considered as a prototypical biomolecule, there are reports on large variation in the position of molecular orbitals, ranging from metallic to insulating characteristics as indicated by the line in the right hand side of the Fig. 6(b) (Stutzmann et al., 2006; Sugiyama and Saito (1996) and Markus et al., 2009). Moreover, efficient and direct transfer of charge carriers between semiconductor substrates and bioorganic layers are pivotal conditions towards systematic detection of specific bio-events by means of band alignment of the relevant electronic levels of the hybrid interface. When a NW electrode meets bioorganic layer, an IDP layer develops at the interface because of relevant molecular band offset leading to the formation of a space charge region below the semiconductor surface [Fig. 6(b)]. In thermodynamic equilibrium, this process results in band bending in upward direction for an intrinsically *n*-type GaN NWs used in this present study. The subsequent chemical modifications and DNA immobilization on the NW surface increase the number of carriers that influence the widening of IDP layer followed by band bending at the interfacial region. During the hybridization process, there is a substantial change in ct-DNA concentration dependent IDP layer as well as upward band bending at the NW surface. These properties at the interface of semiconductor/bioorganic layers act as characteristic basis for DNA sensing in the EIS spectroscopic technique.

A comparative data of the absolute position of valance and conduction band edges for most used semiconductor to that of LUMO and HOMO levels of some organic materials (polymers and DNA) reveal that wide band gap semiconductors (GaN and other group III alloys, ZnO, SiC and diamond) can be ideal to make better electronic contact than that of classical semiconductors such as Si and GaAs (Van de Walle and Neugebauer, 2003 and Stutzmann et al., 2006). It was found that GaN and its alloys with Al can cover a wide range of HOMO or LUMO positions in several bioorganic systems whereas most acclaimed and popular materials like Si or GaAs exhibits a considerable offset in the position of their band gaps. In this context, GaN NWs, being a direct wide band gap semiconductor with narrow conduction channels, are expected to be advantageous as a transducer to read out the bio-event effectively by choosing appropriate physiological conditions and linker molecules.

5. Conclusion

In summary, PAMAM dendrimer modified GaN NWs provide an unprecedented opportunity in realizing ultra-sensitive label-free electrochemical DNA biosensor. By taking the advantage of PAMAM dendrimer comprises of high density of docking sites for p-DNA immobilization and narrow conduction channel of GaN NWs as transducer for the readout system, we have achieved an ultra-low detection limit down to 0.1 aM t-DNA solution. Comparative in-situ studies on single and triplet base pair mismatched, γ-irradiated and complementary t-DNA in the hybridization process reveal selectivity and specificity of the p-DNA/PAMAM/GAN NWs sensor probe. During the hybridization process, there is a substantial change in ct-DNA concentration dependent interfacial polarization resistance, which forms the basis of the present DNA biosensor.

Acknowledgment

We thank M. Kamarudin SND, IGCAR for FESEM studies and S. Dash, SND, IGCAR for general support and encouragement.

Appendix A. Supporting information

Supplementary data associated with this article can be found in the online version at http://dx.doi.org/10.1016/j.bios.2013.01.023.

References

Bonanni, A., Pividori, M.I., Valle, M.D., 2010. Analyst 135, 1765.
Chen, C.P., Ganguly, A., Lu, C.Y., Chen, T.Y., Kuo, C.C., Chen, R.S., Tu, W.H., Fischer, W.B., Chen, K.H., Chen, L.C, 2011. Analytical Chemistry 83, 1938.
Chen, C.P., Ganguly, A., Wang, C.-H., Hsu, C.-W., Chattopadhyay, S., Hsu, Y.-K., Chang, Y.-C., Chen, K.-H., Chen, L.C., 2009. Analytical Chemistry 81, 36.
Chen, Z-W., Balamurugan, A., Chen, S-M., 2009. Bioelectrochemistry 75, 13.
Cui, Y., Wei, Q., Park, H., Lieber, C.M., 2001. Science 293, 1289.
Daniels, J.S., Pourmand, N., 2007. Electroanalysis 12, 1239.
Feigel, I.M., Vedala, H., Star, A., 2011. Journal of Materials Chemistry 21, 8940.
Grieshaber, D., MacKenzie, R., Voros, J., Reimhult, E., 2008. Sensors 8, 1400.
Kang, B.S., Pearton, S.J., Chen, J.J., Ren, F., Johnson, J.W., Therrien, R.J., Rajagopal, P., Roberts, J.C., Piner, E.L., Linthicum, K.J., 2006. Applied Physics Letters 89, 122102.
Lao, C., Li, Y., Wong, C.P., Wang, Z.L., 2007. Nano Letters 7, 1323.
Li, G., Li, X., Wan, J., Zhang, S., 2009. Biosensors and Bioelectronics 24, 3281.
Lisdat, F., Schafer, D., 2008. Analytical and Bioanalytical Chemistry 391, 1555.
Markus, T.Z., Daube, S.S., Naaman, R., Fleming, A.M., Muller, J.G., Burrows, C.J., 2009. Journal of the American Chemical Society 131, 89.
Patolsky, F., Lieber, C.M., 2005. Materials Today 8, 20.
Pérez, E.M., Arya, S.K., Bhansali, S., 2011. Analyst 136, 1686.
Peng, H., Zhang, L., Soeller, C., Travas-Sejdic, J., 2009. Biomaterials 30, 2132.
Ren, F., Pearton, S.J., Kang, B.S., Chu, B.H., 2011. Environment and Biosecurity, ISBN: 978-953-307-443-6, InTech, DOI: 10.5772/16693.
Ramanaviciene, A., Ramanavicius, A., 2004. Analytical and Bioanalytical Chemistry 379, 287.
Sahoo, P., Dhara, S., Amirthapandian, S., Kamruddin, M., Dash, S., Tyagi, A.K., 2012. Crystal Growth and Design 12, 2375.
Sahoo, P., Dhara, S., Das, C.R., Dash, S., Tyagi, A.K., Raj, B., 2010. International Journal of Nanotechnology 7, 7823.
Sahoo, P., Dhara, S., Dash., S., Tyagi, A.K., 2011a. Nanoscience and Nanotechnology-Asia 1, 140.
Sahoo, P., Oliveira, D.S., Cotta, M.A., Dhara, S., Dash, S., Tyagi, A.K., Raj, B., 2011b. Journal of Physical Chemistry C 115, 5863.

Stutzmann, M., Garrido, J.A., Eickhoff, M., Brandt, M.S., 2006. Physica Status Solidi (a) 203, 3424.
Sugiyama, H., Saito, I., 1996. Journal of the American Chemical Society 118, 7063.
Synytsya, A., Alexa, P., Boer, J.d., Loewe, M., Moosburger, M., Wurkner, M., Volka, K., 2007. Journal of Raman Spectroscopy 38, 1406.
Teles, F.R.R., Fonseca, L.P., 2008. Materials Science and Engineering **C** 28, 1530.
Van de Walle, C.G., Neugebauer, J., 2003. Nature423627
Wanekaya, A.K., Chen, W., Myung, N.V., Mulchandani, A., 2006. Electroanalysis 18, 533.
Wang, J., 2006. Biosensors and Bioelectronics 21, 1887.
Wang, R., Sheng, Z-M., Taubenberger, J.K., 2009. Journal of Clinical Microbiology 47, 2675.
Wang, W.U., Chen, C., Lin, K-H., Fang, Y., Lieber, C.M., 2005. Proceedings of the National Academy of Sciences 102, 3208.
World Health Organization, Swine influenza, 2009. Weekly Epidemiological Record 84, 149.
Yang, Y., Sugimoto, J.D., Halloran, M.E., Basta, N.E., Chao, D.L., Matrajt, L., Potter, G., Kenah, E., Longini Jr, I.M., 2009. Science 326, 729.
Zhu, N., Gao, H., Xu, Q., Lin, Y., Su, L., Moa, L., 2010. Biosensor and Bioelectronics 25, 1498.
Zhu, N., Gu, Y., Chang, Z., He, P., Fang, Y., 2006. Electroanalysis 18, 2107.